Published by IOP Publishing for Sissa Medialab

Received: *May 30, 2025*
Accepted: *July 7, 2025*
Published: *August 27, 2025*

20th Anniversary Trento Workshop on Advanced Silicon Radiation Detectors
Trento, Italy
4–6 February 2025

The SiPM photodetector of the ePIC dual-radiator RICH at the EIC: overview and beam test results

B Rajesh Achari[a,h,*] **N. Agrawal**[a,h] **M. Alexeev**[c,l] **C. Alice**[c,l] **P. Antonioli**[a] **C. Baldanza**[a] **L. Barion**[b] **A. Calivà**[e,p] **M. Capua**[d,o] **M. Chiosso**[c,l] **M. Contalbrigo**[b] **F. Cossio**[c] **M. Da Rocha Rolo**[c] **A. De Caro**[e,p] **D. De Gruttola**[e,p] **G. Dellacasa**[c] **D. Falchieri**[a] **S. Fazio**[d,o] **N. Funicello**[e,p] **M. Garbini**[a,g] **S. Geminiani**[a,h] **M. Giacalone**[a] **D. Giordano**[c] **R. Malaguti**[b] **F. Mammoliti**[m] **M. Mignone**[c] **C. Mingioni**[c] **M. Nenni**[c] **F. Noto**[m] **L. Occhiuto**[d,o] **A. Paladino**[a] **D. Panzieri**[c,n] **L. Polizzi**[b] **R. Preghenella**[a] **L. Rignanese**[a] **C. Ripoli**[e,p] **E. Rovati**[a,h] **N. Rubini**[h] **M. Ruspa**[c,n] **U. Tamponi**[c] **E. Tassi**[d,o] **C. Tuvè**[f,q] **S. Vallarino**[i] **and R. Wheadon**[c]

[a] *INFN Sezione di Bologna, Bologna, Italy*
[b] *INFN Sezione di Ferrara, Ferrara, Italy*
[c] *INFN Sezione di Torino, Torino, Italy*
[d] *INFN Gruppo Collegato di Cosenza, Cosenza, Italy*
[e] *INFN Gruppo Collegato di Salerno, Salerno, Italy*
[f] *INFN Sezione di Catania, Catania, Italy*
[g] *Museo Storico della Fisica e Centro Studi e Ricerche Enrico Fermi, Rome, Italy*
[h] *Università degli Studi di Bologna, Bologna, Italy*
[i] *INFN Sezione di Genova, Genova, Italy*
[l] *Università degli Studi di Torino, Torino, Italy*
[m] *INFN Laboratori Nazionali del Sud, Catania, Italy*
[n] *Università del Piemonte Orientale, Vercelli, Italy*
[o] *Università degli Studi della Calabria, Rende, Italy*
[p] *Università degli Studi di Salerno, Salerno, Italy*
[q] *Università degli Studi di Catania, Catania, Italy*

E-mail: brajesh.achari@unibo.it

Abstract: The dual-radiator RICH (dRICH) detector of the ePIC experiment at the upcoming Electron-Ion Collider (EIC) will use silicon photomultipliers (SiPMs) for single-photon detection of Cherenkov light. Several novel INFN driven modular prototype photodetections units (PDUs)

*Corresponding author.

https://doi.org/10.1088/1748-0221/20/08/C08025

2025 JINST 20 C08025

have been constructed, each integrating 256 SiPMs, cooling infrastructure and front-end electronics. To achieve a large area coverage, eight PDUs were assembled totalling 2048 readout channels; the full system was then tested at the CERN-PS T10 beamline. The system operated reliably under realistic conditions, and particle identification performance was validated over momenta ranging from 2 to 11 GeV/c using different radiator configurations. Complementary to the testing of sensor on the beam test lines, R&D is also ongoing to ensure consistent performance under radiation exposure. In-situ annealing methods using forward-bias heating have been developed to recover radiation damage of SiPMs. These techniques proved effective, with a recovery of radiation-induced damage up to 97–98% as observed in reducing the dark current. The effects of these procedure on the photo-detection efficiency of the sensors was also tested. Through repeated annealing cycles at different temperatures, a yellowing of the SiPM window has been noticed in the 175 °C batch, the origin of this effect is still under investigation.

KEYWORDS: Cherenkov detectors; Particle identification methods; Photon detectors for UV, visible and IR photons (solid-state)

2025 JINST 20 C08025

Contents

2025 JINST 20 C08025

1 Introduction

The Electron-Ion Collider (EIC) [1, 2], currently being developed at Brookhaven National Laboratory, is an upcoming facility that will allow researches to explore the inner structure of nucleons and nuclei. By colliding polarized electrons with polarized protons and ions over a range of 20 to 140 GeV of center-of-mass energies, the EIC will provide high-precision data to investigate fundamental questions in quantum chromodynamics (QCD), including the distribution of gluons and sea quarks and the origin of nucleon spin. The ePIC experiment consists of a general-purpose detector, which includes a dual-radiator Ring Imaging Cherenkov (dRICH) detector designed to provide charged hadron separation in the forward region, covering pseudorapidities between approximately 1.5 and 3.5. To cover a wide range of momenta ($\sim$ 3 to 50 GeV/c), the dRICH uses a combination of aerogel and gas radiators [2].

The readout of Cherenkov light will rely on silicon photomultipliers (SiPMs) [2, 3], which are compact, cost-effective and unaffected by strong magnetic fields, which are foreseen in the dRICH region ($\sim$ 1 T). However, SiPMs are not radiation hard [4, 5], the main drawback being the increase dark count rates (DCR) and degradation of single-photon detection. This presents a significant challenge for long-term operation and requires active strategies (e.g., low-temperature operation, precise timing electronics and high-temperature annealing, etc.) to mitigate radiation effects and preserve performance [6].

To evaluate and validate the system design, we constructed a prototype dRICH detector composed of eight novel PhotoDetection Units (PDUs) [7], each integrating 256 SiPMs with a pixel size of $3 \times 3\,\mathrm{mm}^2$ and an ALCOR-based front-end readout electronics [8, 9]. This prototype was tested at the T10 beamline of CERN Proton Synchrotron, enabling us to study the performance of the readout system under realistic experimental conditions.

This paper will place particular emphasis on the in-situ online annealing method by measuring the dark current and relative photon detection efficiency (PDE) at different annealing configurations, followed by a brief overview of the key findings from the 2024 beam test campaign.

2 Radiation damage and annealing studies

During the years of operation of the EIC, the dRICH is expected to receive an integrated luminosity of 1000 fb^{-1} corresponding to an integrated 1 MeV neutron equivalent fluence ($\mathrm{n_{eq}}$) of $\sim 6\times10^{10}\,\mathrm{cm}^{-2}$ [6].

To evaluate the radiation hardness and potential for recovery, the sensors have been exposed to various radiation doses up to 1×10^{11} $n_{eq}cm^{-2}$, which considers a safety margin with respect to the expected fluence. The irradiation was performed in the Trento Proton Therapy Centre, Italy in collaboration with Trento Institute for Fundamental Physics and Applications (TIFPA), using their proton beam energy ranging from 18 to 138 MeV and scaled based on Non-Ionising Energy Loss (NIEL) hypothesis. The increase of DCR was observed to be in line with previous results, indicating a linear trend with dose [6]. As probe for radiation damage, we have measured both the increase in dark current and the degradation of pseudo-photodetection efficiency (pPDE), all measurements were performed at −30 °C, unless specified otherwise.

2.1 Dark current

The first studies were performed subjecting the proton-irradiated sensors to a 150 °C annealing lasting 200 hours, using an oven to deliver the heat. This result has then been used as the benchmark target in terms of recovery, achieving 97–98% recovery of dark current generated by the radiation [6]. Since it is impractical to dismount the SiPMs for oven-based annealing in a real experimental setup, an online in-situ annealing technique was developed using forward bias to locally heat up the sensors. This method leverages the internal power dissipation of the SiPMs under forward bias to reach the desired annealing temperatures without removing them from the detector. The temperature of each SiPM is calibrated as a function of the applied forward current, using an Arduino-based control system that receives feedback from a FLIR infrared thermal monitoring camera. It was observed that a maximum power dissipation of approximately 1 W per sensor is sufficient to reach a temperature more than 175 °C. The experimental setup is shown in figure 1 (right).

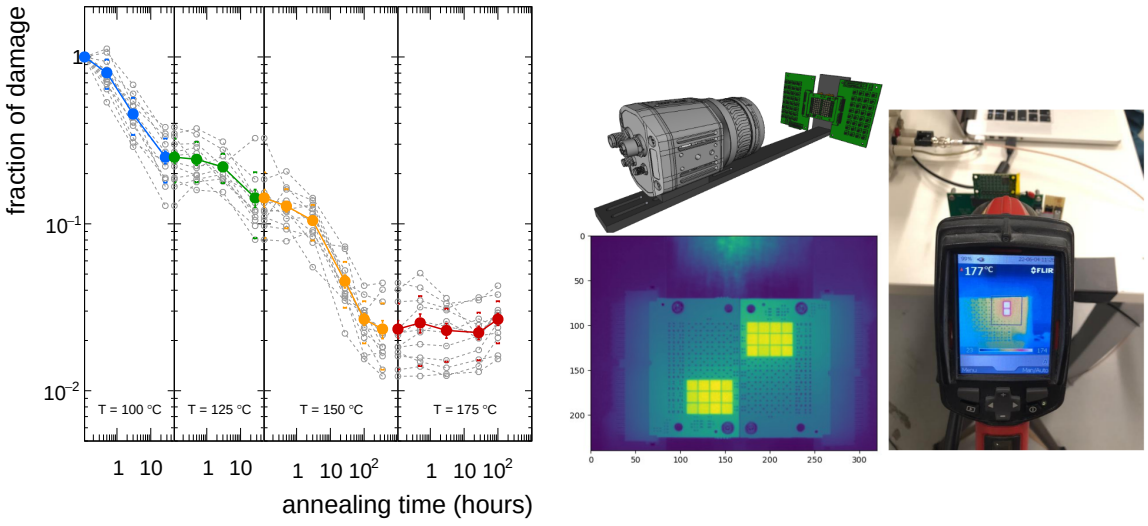

Figure 1. Left: fractional damage of SiPM with respect to annealing hours for different temperature steps (different colors) The gray line is due to different sensors and the solid colored line indicates averaging over them. Middle and top: the CAD model [10] of a thermal imaging camera focused onto a annealing SiPM board to monitor the SiPM's temperature. Reproduced with permission from [10]. Middle bottom: image taken by the FLIR [10] camera during annealing. Right: the experimental setup during online in-situ annealing.

As a first exploration of direct current annealing, data were taken at increasing annealing temperature. The test started at 100 °C and increased the temperature in 25 °C steps, up to 175 °C.

2025 JINST 20 C08025

This configuration was studied considering the effectiveness in reducing the dark current of the SiPMs while keeping in mind the thermal contacts and physical constraints of the detector. Also to verify the consistency of the annealing procedure, multiple SiPMs were subjected to identical annealing conditions. The observed behavior was consistent across them, with similar levels of dark current recovery. As a result, the data from these SiPMs were averaged to obtain the final performance as indicated with solid coloured lines as shown in figure 1 (left). The results also showed that annealing at 150 °C for 100 hours was sufficient to recover approximately 97% of the radiation-induced damage. However, going beyond 150 °C temperature after 300 h has no significant improvement in the dark current and ultimately it saturates after that.

2.2 Relative photodetection efficiency

To evaluate the impact of radiation damage and annealing on the photon detection capability of the SiPMs, a pulsed-laser setup was employed to measure the relative PDE. A laser light at 400 nm was directed onto the SiPM sensors, which were coupled to prototype ALCOR-based readout electronics and placed inside a climatic chamber operating at −30 °C. A neutral-density filter system attenuated the laser to ensure single-photon conditions, with the pulse intensity adjusted so that fewer than 1% of the laser pulses resulted in a detected signal.

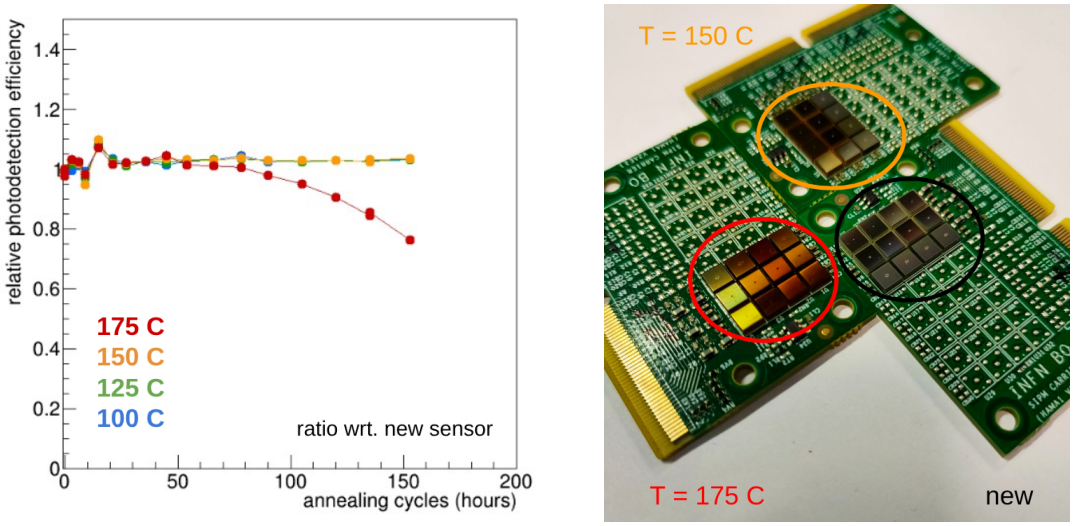

Figure 2. Left: relative photo detection efficiency measured after different annealing cycles for different annealing temperature. Right: a yellow discolouration on the window of annealed SiPM board (encircled in red) can be seen compared to new SiPM board (encircled in black).

As the laser output remained constant across all tests, the number of detected photon events after each annealing condition served as an estimate of the PDE. This value was then normalized to the PDE of a non-irradiated reference SiPM to determine the relative PDE. Measurements were conducted across different annealing temperatures and durations, with the results summarized in figure 2 (left).

After approximately 500 hours of annealing at 175 °C, a yellow discolouration was observed on the SiPM window as can be seen in figure 2 (right), which correlated with a noticeable drop in relative PDE as shown in figure 2 (left). This effect was not present in sensors annealed at lower temperature. It was also not observed in sensors annealed in the oven at similar temperatures and integrated times.

2025 JINST 20 C08025

The cause of the discolouration is still under investigation. One hypothesis that is currently being explored is that the prolonged high-temperature annealing in open air allowed atmospheric gases or humidity to alter the chemical composition of the sensor window.

To prevent this in future tests, a new in-situ annealing setup is being developed. This system will enclose the SiPMs in a sealed chamber with a controlled dry air environment to maintain zero humidity during high-temperature cycles.

3 dRICH prototype and beam tests

To evaluate the performance of the dRICH detector and its associated electronics under conditions close to the final design, several beam tests were conducted at the CERN-PS in 2022, 2023, and 2024. Each test focused on a different aspect of the detector system. The 2022 beam test aimed to validate the performance of the SiPMs in a realistic radiation environment using an ALCOR prototype chip [3, 8]. In 2023, the prototype was equipped with 1280 readout channels based on a upgraded ALCOR chip, with the goal of detecting and reconstructing the complete Cherenkov ring under various voltage and ALCOR configurations [11]. In the most recent 2024 test, the prototype was upgraded to 2048 readout channels and used an further improved version of the ALCOR chip.

3.1 dRICH prototype

The dRICH prototype is based on a modular, compact and novel photodetection unit (PDU). Each PDU contains photosensors covering approximately $5 \times 5\,\mathrm{cm}^2$ area, front-end electronics, and a cooling plate, as shown in figure 3 (left). Eight PDUs were arranged along the edges of a 3×3 square, leaving the center open to place an aerogel radiator tile and allow an unobstructed beam path, as shown in figure 3 (right).

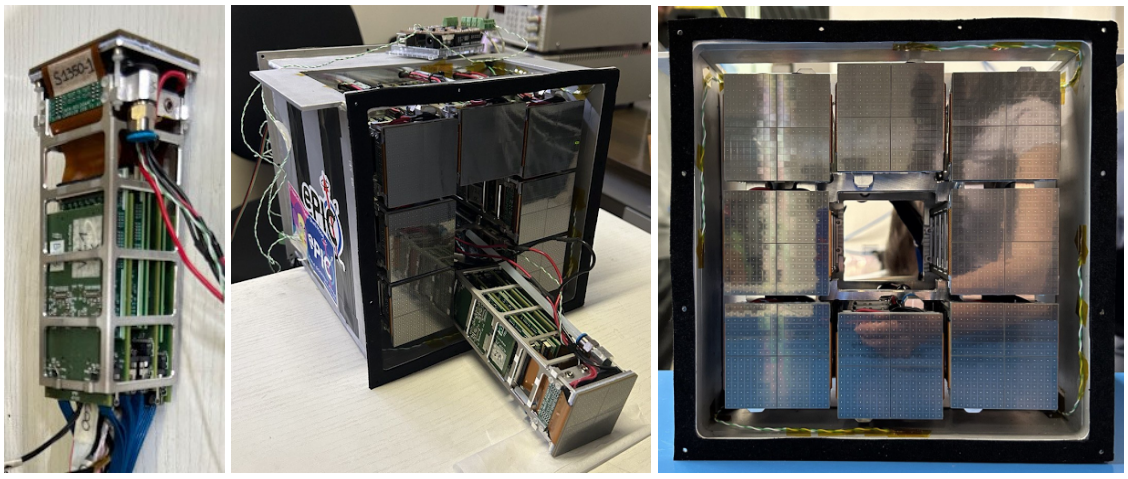

Figure 3. Left: picture of a PDU showing SiPMs on the top and front-end electronics below. Middle: dRICH prototype readout box showing the arrangement of PDUs prior to the final installation. Right: completed readout box showing the full SiPM array for Cherenkov light detection.

The prototype vessel [12] was designed to accommodate the gas radiators and mirrors to generate and focus Cherenkov light, as illustrated in figure 4 (left). Particles first pass through an aerogel tile ($n \approx 1.02$) placed at the front. The Cherenkov photons produced are reflected back by the first spherical

2025 JINST 20 C08025

concave mirror, located approximately 340 mm from the radiator. The filled C_2F_6 gas ($n \approx 1.008$) inside the enclosure vessel act as a second radiator for the particles. The photons from this radiator are reflected by a second mirror, located approximately at 1200 mm. A slider mechanism is also there which allows to adjust the position of mirrors along the light path. The reflected Cherenkov light is detected by the photodetector array, producing the rings shown in figure 4 (right). As expected from their refractive indices, the aerogel with higher refractive index ($n \approx 1.02$) produces a larger Cherenkov angle than the C_2F_6 gas with lower refractive index ($n \approx 1.008$). As a result, the outer ring corresponds to the aerogel radiator, while the inner ring is produced by the gas radiator. One ALCOR chip (32 channels) was non-functional due to a front-end issue, resulting in missing hits in that region. Despite this, the results clearly demonstrate successful beam test operation of the dRICH prototype.

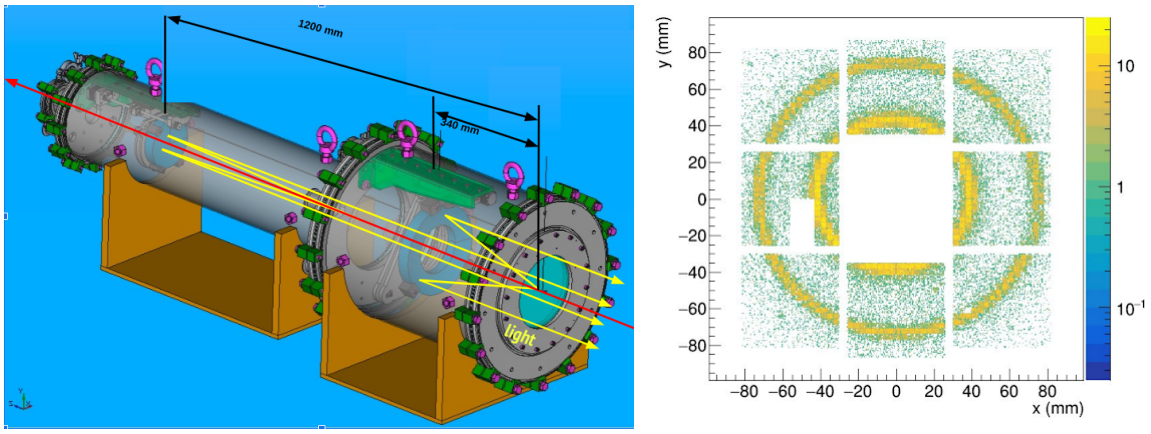

Figure 4. Left: schematic of the dRICH prototype showing the path of Cherenkov light. Right: sample image showing Cherenkov rings produced by both radiators. The inner rings corresponds to gas radiator and outer is by aerogel radiator.

During the campaign, all subsystems — including power, cooling, data readout, and sensor biasing — were operated under realistic conditions to assess system readiness. Thermal regulation of the SiPMs and front-end electronics was achieved using a hybrid system combining liquid cooling plates and Peltier modules mounted within each PDU. The setup maintained operational temperatures down to −40 °C during beam tests to suppress dark noise. The front-end electronics based on the ALCOR chip were configured using commercial Xilinx FPGA boards. These boards controlled timing, and data flow, and interfaced with the DAQ system via optical links. During the beam tests, synchronization with the beam trigger and timing calibration across channels were performed to ensure coherent event reconstruction. The system achieved stable operation at high channel density (2048 channels), and data integrity was verified through online monitoring and offline analysis. The robustness of the system under operational loads confirms its suitability for integration in the full dRICH detector.

3.2 Results of beam test 2024

A primary objective of the 2024 beam test was to study particle identification performance over a broad momentum range using different radiator configurations. Data were collected at momenta from 2 GeV/c to 11 GeV/c in 1 GeV/c steps and with various radiator materials, as shown in figure 5 (left). The reconstructed signal closely matched the expected distributions, validating the ability of the detector to distinguish protons, kaons and pions from each other and confirming its readiness for future application. No data were collected at 9 GeV/c due to a beam configuration error.

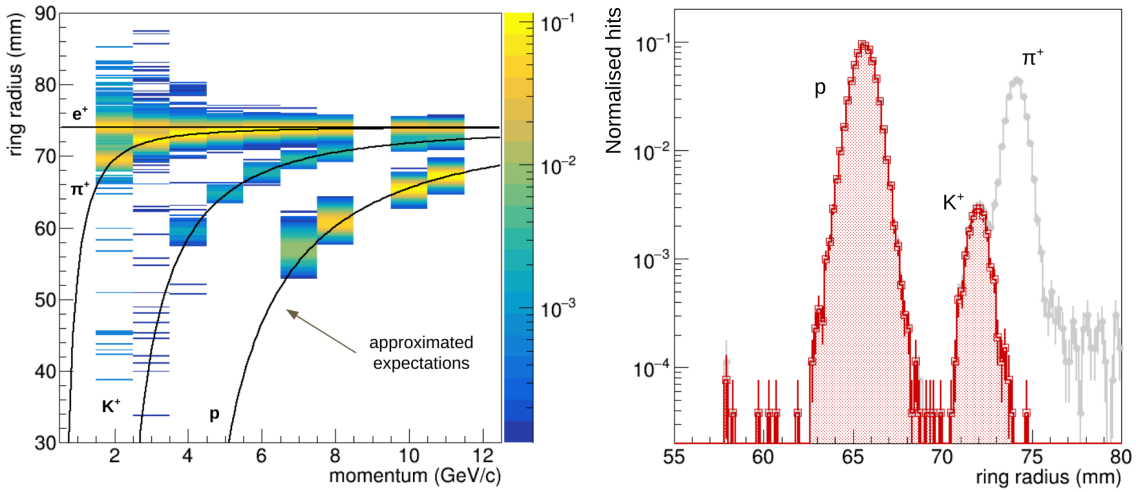

Figure 5. Left: reconstructed aerogel ring radius from momentum scan. The solid lines indicate the expectations for various particle mass hypothesis. Right: reconstructed aerogel ring radius showing particle separation at 10 GeV/c beam momentum. The shaded regions shows the events generated due to only aerogel radiator, however, the unshaded regions show the events generated due to both the radiators. Reproduced from [7]. The Author(s). CC BY 4.0.

Figure 5 (right) shows the normalized distribution of photon hits from the aerogel radiator for a positive beam at 10 GeV/c. The proton peak is clearly separated from the pion and kaon peaks; however, at this momentum, the kaon distribution begins to overlap with that of the pions. In the gas region at this energy, only pions produce Cherenkov light, as both kaons and protons are below the Cherenkov threshold. This allows the gas ring to serve as a pion tag, enabling a clean identification of the kaon peak from the aerogel ring, as illustrated by the shaded area in figure 5 (right). The combined use of aerogel and gas radiators effectively separates hits from protons, kaons, and pions, demonstrating the dual-radiator capability of the detector.

4 Conclusions

Significant progress was made in radiation damage mitigation through in-situ forward-bias annealing, with up to 97–98% recovery of dark current achieved under controlled conditions. The method was validated across a range of annealing temperatures and durations. An unexpected yellowing of the SiPM windows was observed after extended annealing at 175 °C, which is currently under further investigation. Future annealing tests will use sealed, low-humidity enclosures to evaluate the causes of this effect.

The successful beam test at CERN-PS demonstrates the operation of a modular 2024 channels of SiPM-based Cherenkov photodetector. The test validated the performance of the photodetection units, confirming their ability to operate at low temperature and integration with front-end electronics to mitigate the DCR. The results also demonstrated effective particle identification across a broad momentum range (2–11 GeV/c), achieved through the combined use of aerogel and gas radiators, in line with the physics goals of the ePIC experiment.

Ongoing efforts will focus on refining the annealing technique, improving readout electronics, and finalizing the system design. In next years, we aim to build and test the final dRICH prototype, leading to design optimizations and eventual large-scale production for deployment in the ePIC experiment.

2025 JINST 20 C08025

Acknowledgments

This work is funded by the Commissione Scientifica Nazionale 3 (CSN3) of the Istituto Nazionale di Fisica Nucleare, Italy. This project has also received funding from the European Union's Horizon 2020 Research and Innovation programme under GA no 101004761 and GA no 824093. This work is supported by the U.S. Department of Energy, Office of Science, Office of Nuclear Physics under the EIC project number JSA-22-R412967. The authors would like to thank the CERN PS operation teams and TIFPA staffs for their help during the beam tests and irradiation campaigns respectively.

References

[1] R. Abdul Khalek et al., *Science Requirements and Detector Concepts for the Electron-Ion Collider: EIC Yellow Report*, *Nucl. Phys. A* **1026** (2022) 122447 [arXiv:2103.05419].

[2] T. Ullrich, *Requirements and R&D for detectors at the future Electron-Ion Collider*, *Nucl. Instrum. Meth. A* **1039** (2022) 167041.

[3] R. Preghenella et al., *SiPM photosensors for the ePIC dual-radiator RICH detector at the EIC*, *PoS* **EPS-HEP2023** (2024) 515.

[4] E. Garutti and Y. Musienko, *Radiation damage of SiPMs*, *Nucl. Instrum. Meth. A* **926** (2019) 69 [arXiv:1809.06361].

[5] L.P. Rignanese, P. Antonioli, R. Preghenella and E. Scapparone, *SiPMs and examples of applications for low light detection in particle and astroparticle physics*, *Riv. Nuovo Cim.* **47** (2024) 299.

[6] R. Preghenella et al., *Study of radiation effects on SiPM for an optical readout system for the EIC dual-radiator RICH*, *Nucl. Instrum. Meth. A* **1056** (2023) 168578.

[7] R. Preghenella et al., *Beam test results of the SiPM photodetector prototype for the ePIC-dRICH detector at the EIC*, 2025 *JINST* **20** C07005.

[8] F. Cossio et al., *ALCOR: A mixed-signal ASIC for the dRICH detector of the ePIC experiment at the EIC*, *Nucl. Instrum. Meth. A* **1069** (2024) 169817.

[9] DarkSide collaboration, *Integrated front-end electronics for single photon time-stamping in cryogenic dark matter detectors*, 2020 *JINST* **15** C05019.

[10] FLIR Systems, Inc., *Flir a400/a500/a700 series smart sensor and imaging camera*, (2022), https://www.flir.it/products/a400-a700-science-kits/?model=91903-0102&vertical=rd+science&segment=solutions.

[11] C. Alice et al., *A large-area SiPM readout plane for the ePIC-dRICH detector at the EIC: Realisation and beam test results*, *Nucl. Instrum. Meth. A* **1068** (2024) 169669.

[12] S. Vallarino et al., *Prototype of a dual-radiator RICH detector for the Electron-Ion Collider*, *Nucl. Instrum. Meth. A* **1058** (2024) 168834.

2025 JINST 20 C08025